Clays and Clay Minerals, Vol. 41, No. 1, 103–110, 1993.

DEVELOPMENT OF AMMONIUM-SAPONITES FROM GELS WITH VARIABLE AMMONIUM CONCENTRATION AND WATER CONTENT AT LOW TEMPERATURES*

J. THEO KLOPROGGE,[1]** JOHAN BREUKELAAR,[2] J. BEN H. JANSEN,[1]*** AND JOHN W. GEUS[3]

[1] Department of Geochemistry, Institute of Earth Sciences, University of Utrecht, Budapestlaan 4, P.O. Box 80.021, 3508 TA Utrecht, The Netherlands

[2] Koninklijke/Shell-Laboratorium Amsterdam (Shell Research B.V.), P.O. Box 3003, 1003 AA Amsterdam, The Netherlands

[3] Department of Inorganic Chemistry, University of Utrecht, P.O. Box 80.083, 3508 TB Utrecht, The Netherlands

Abstract—Ammonium-saponite is hydrothermally grown at temperatures below 300°C from a gel with an overall composition corresponding to $(NH_4)_{0.6}Mg_3Si_{3.4}Al_{0.6}O_{10}(OH)_2$. The synthetic saponite and coexisting fluid have been characterized by means of X-ray powder diffraction, X-ray fluorescence, Induced Coupled Plasma-Atomic Emission Spectroscopy, thermogravimetric analysis, transmission electron microscopy, CEC determination using an ammonia selective electrode, and pH measurement. In the crystallization model developed, crystallization started with the growth of individual tetrahedral layers with an aluminum substitution not controlled by the Al^{IV}/Al^{VI} ratio in the gel and hydrothermal fluid, on which the octahedral Mg layers can grow. During the synthesis, individual sheets stacked to form thicker flakes while lateral growth also took place. The remaining Al^{VI} partly replaced ammonium as the interlayer cation.

Key Words—Cation exchange capacity, Infrared spectroscopy, Saponite, Synthesis, Thermal analysis, Transmission electron microscopy, X-ray powder diffraction.

INTRODUCTION

During the last ten years, interest in the use of smectites as catalysts and molecular sieves has increased. Synthetic clays, such as beidellite (Plee *et al.*, 1987; Schutz *et al.*, 1987; Kloprogge *et al.*, 1990a, 1990b; Kloprogge, 1992), hectorite, and fluorhectorite (Shabtai *et al.*, 1984; Sterte and Shabtai, 1987; Torii and Iwasaki, 1987), are preferred to natural smectites because of their high purity and their adjustable composition; however, synthetic saponites have so far not received much attention, even though they exhibit a higher (hydro)thermal stability than other smectites.

Only a few studies have been devoted to the synthesis of Na-saponites. Koizumi and Roy (1959) and Iiyama and Roy (1963) used as starting material a gel consisting of nitrates of aluminum, magnesium, and sodium in combination with Ludox AS, a commercial colloidal silica suspension stabilized by ammonium. Suquet *et al.* (1977) and Lipsicas *et al.* (1984) prepared a gel according to the procedure described extensively by Hamilton and Henderson (1968). Hickson (1974, 1975a and 1974b) made an aqueous slurry of hydrous alumina, magnesia, and silica within ammonium hydroxide, while Iwasaki *et al.* (1989) dissolved magnesium chloride and aluminum chloride in an acidified sodium silicate solution that was subsequently mixed with an alkali solution. All these syntheses have in common that they were performed at temperatures and pressures ranging from 150° to 450°C and autogeneous water pressure to 1500 bar, respectively. An exception is the method described by Decarreau (1980, 1985), who precipitated saponite nuclei at room temperature from sodium silicate and sodium aluminate in a solution of a magnesium salt acidified with the corresponding acid. These nuclei were aged for three weeks in water at temperatures between 5° and 90°C.

The aim of this study is to provide a precise characterization of synthetic ammonium-saponites from gels with variable ammonium concentrations and water content in the temperature range 125° to 280°C.

EXPERIMENTAL METHODS

The gel was prepared from a homogeneous mixture of stoichiometric amounts of powders of amorphous silica (SiO_2, Baker 0254), aluminiumtriisopropylate ($Al[OCH(CH_3)_2]_3$, Merck 801079), and magnesium-acetate-tetrahydrate [$(CH_3COO)_2Mg \cdot 4H_2O$], Merck 5819). The powder mixture was brought into aqueous ammonium hydroxide solutions (NH_4OH, Baker 6051) to produce a saponite with a theoretical composition of $(NH_4)_{0.6}Mg_3Al_{0.6}Si_{3.4}O_{10}(OH)_2$. Approximately 125 g of the gel were hydrothermally treated in a 250 ml autoclave for 72 hr at temperatures between 125° and 280°C and autogeneous water pressure. After cooling,

* This paper is a joint contribution from the Debye Institute, University of Utrecht, The Netherlands, and Shell Research B.V., Amsterdam.

** Present address: Plastics and Rubber Institute TNO, P.O. Box 108, 3700 AC Zeist, The Netherlands.

*** Present address: Bowagemi, Prinses Beatrixlaan 20, 3972 AN Driebergen, The Netherlands.

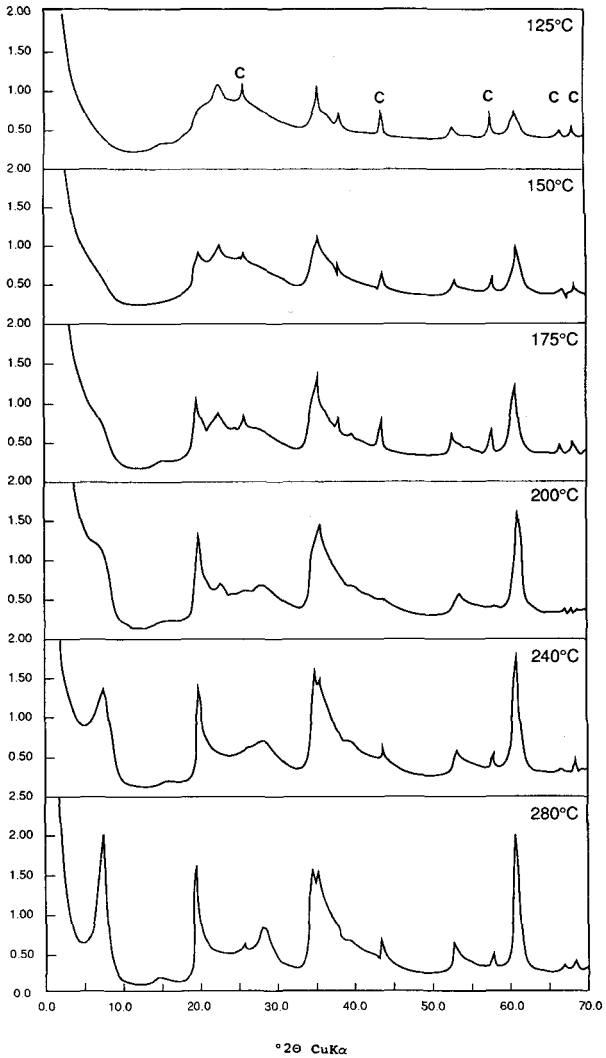

Figure 1. X-ray powder diffraction patterns of saponites synthesized at different temperatures (series 2); c = corundum.

the solid product was washed twice with demineralized water followed by an ion-exchange with a 1 M ammoniumchloride solution at room temperature to ensure that all exchangeable sites were occupied by ammonium. Finally, the solid product was washed another three times, sedimented by centrifugation, and dried overnight at 120°C. A sieve fraction <64 μm was used for characterization, on the assumption that any amorphous material present would have a particle size >64 μm (based on unpublished data by the Koninklijke/Shell Laboratorium Amsterdam).

After synthesis, the pH of the coexisting hydrothermal liquid was measured as well as that of the water after washing the resulting solid once with 2 L water. X-ray powder diffraction (XRD) patterns were recorded with a Philips diffractometer equipped with PW 1700 hardware and APD1700 software and using CuKα radiation. Thermogravimetric and differential thermal analyses (TGA/DTA) were made with a Du Pont 1090 Thermal Analyzer using heating rates of 10°C/min and 20°C/min, respectively.

Table 1. X-ray powder diffraction data for synthetic NH_4-saponite obtained with a diffractometer (CuKα radiation).

d(obs)[1]	I/I_{max}[1] (%)	Indices[2]	d[2] Ca	d[3] Na	Intensity[2,4]
12.34	87	001	15.29	12.6	vvvs
		002	7.65	6.3	w
4.58	72	020/110	4.61		vs
3.24	24	113	3.256		vw
2.60	84	−202	2.598		m
2.55	84	201	2.560		s
2.38	1	202	2.418		s
1.738	11	−311	1.7454		m
		−242	1.7259		vw
1.529	100	060	1.5389		vvs
		−332	1.5320		vs

[1] NH_4-saponite from run HTSAP2b (240°C, NH_4/Al = 1.0, H_2O/(Si + Al) = 10).
[2] Two-water layer Kozákov saponite (Guinier de Wolff camera) (Suquet *et al.*, 1975).
[3] Na-exchanged Kozákov saponite (Suquet *et al.*, 1975).
[4] v = very; s = strong; m = medium; w = weak.

Elemental analyses were performed using X-ray fluorescence (XRF). The coexisting hydrothermal fluid was analyzed with Inductively Coupled Plasma (ICP) atomic emission spectrometry. Infrared (IR) absorption spectra were obtained on powdered samples in KBr tablets (sample concentration 1 wt. %) using a Perkin Elmer 580 IR spectrophotometer.

The cation exchange capacity (CEC) of the saponite was determined from the NH_4^+ content in solution after exchange with NaCl using an ammonia-selective electrode. Surface areas of the ammonium saponites were determined using a commercial apparatus from Micromeretics, applying the BET equation. The samples were first calcined at 550°C and subsequently degassed at 300°C in vacuum. Measurements were performed at liquid nitrogen temperature, using nitrogen as the sorbate and assuming the surface area of adsorbed nitrogen to be 16.2 Å^2.

The morphology and particle sizes of the products obtained were investigated with a Philips EM 420 transmission electron microscope (TEM) operated at 120 kV.

RESULTS

The XRD patterns of the solid products display the diffraction pattern of saponite with a small amount (1%-3%) of corundum, α-Al_2O_3 (Figure 1). The corundum is not produced during the synthesis but is an artifact from the mortar in which the powders for the gel preparation were ground. The basal spacings of the saponites vary between 12.08 Å (7.31° 2θ) and 12.35 Å (7.15° 2θ). The intensities and the sharpness of the (001) and (060) reflections increase with increasing syn-

https://doi.org/10.1346/CCMN.1993.0410111 Published online by Cambridge University Press

Table 2. Experimental conditions at autogeneous water pressure for 72 hours, pH after washing, CEC, and BET surface area of the products.

A. Gels with mol ratio $H_2O/(Si + Al) = 10$

Run	NH_4/Al	T (°C)	pH wash	CEC meq/100 g	BET surface area m_2/g
LTSAP1a	0.8	200	4.50	33	—
LTSAP1b	0.8	175	4.74	33	—
LTSAP1c	0.8	150	5.24	27	—
LTSAP1d	0.8	125	5.63	29	—
HTSAP2a	1.0	280	4.58	46	168
HTSAP2b	1.0	240	4.43	53	231
LTSAP2a	1.0	200	4.54	38	348
LTSAP2b	1.0	175	4.74	32	375
LTSAP2c	1.0	150	5.27	33	328
LTSAP2d	1.0	125	5.64	30	248
LTSAP3a	1.2	200	4.61	39	—
LTSAP3b	1.2	175	5.10	35	—
LTSAP3c	1.2	150	5.29	33	—
LTSAP3d	1.2	125	5.62	33	—
LTSAP4a	1.4	200	4.62	45	—
LTSAP4b	1.4	175	5.48	6	—
LTSAP4c	1.4	150	5.28	36	—
LTSAP4d	1.4	125	5.93	32	—

B. Gels with mol ratio $NH_4/Al = 1.0$

Run	$H_2O/Si + Al$	T (°C)	pH wash	CEC meq/100 g	BET surface area m^2/g
LTSAP5a	15	200	4.53	46	—
LTSAP5b	15	175	4.82	33	—
LTSAP5c	15	150	5.33	36	—
LTSAP5d	15	125	5.65	35	—
LTSAP6a	20	200	4.51	47	—
LTSAP6b	20	175	4.81	36	—
LTSAP6c	20	150	5.54	38	—
LTSAP6d	20	125	5.77	37	—
HTSAP7a	25	280	4.47	56	166
HTSAP7b	25	240	4.38	68	333
LTSAP7a	25	200	4.94	44	346
LTSAP7b	25	175	4.87	36	198
LTSAP7c	25	150	5.34	40	314
LTSAP7d	25	125	5.81	37	262

thesis temperature. At synthesis temperatures of 200°C and lower, the (001) reflection can only be distinguished as a shoulder on the intense low angle scattering from the primary X-ray beam.

The (hkl) values of the synthetic NH_4-saponite were indexed according to the values of the Kozákov saponite (Suquet *et al.*, 1975) (Table 1). A discrepancy shows up in the d-values of the reflections with $l \neq 0$ because the presence of ammonium instead of mainly Ca, as the interlayer cation, results in a higher basal spacing (Table 1). After sodium exchange the basal spacing of the Kozákov saponite decreases to 12.6 Å, which is closer to the basal spacing of ammonium-saponite. Upon calcination at 550°C, the basal reflection broadens and exhibits two overlapping maxima at 12.5 Å and 10.2 Å.

Table 2 summarizes the pH of the fluid after washing for the first time as well as the cation exchange capacities (CEC) and the BET surface areas of the solid products obtained. The pH decreases monotonically as the temperature increases from 125° to 200°C. The CEC values never represent more than 45% of the theoretical CEC of 155 meq/100 g calculated from the structural formula assuming a dry product. A decrease in the CEC value is observed with decreasing synthesis temperature at constant water content and initial ammonium concentration. Higher CEC values are obtained with higher ammonium concentrations at the same synthesis temperature. A similar trend is observed with the water content, except for the syntheses performed at 200°C, which show a maximum at a molar $H_2O/(Si + Al)$ ratio of 20. The BET surface areas do not seem to depend on the ammonium concentration or water content. With increasing synthesis temperature, a maximum BET surface area is observed at 175° to 200°C.

TEM illustrates that the hydrothermal product synthesized at 280°C using a molar ratio $H_2O/(Si + Al)$ of 10 (HTSAP2a) consists of a homogeneous mass of small flakes approximately 60 Å thick and 400–800 Å in diameter (Figure 2a). Only a small amount of amorphous material is observed in HTSAP2a. With decreasing synthesis temperature, the amount of amorphous material increases. At 125°C (LTSAP2d), the bulk product consists mainly of amorphous material with only a few saponite flakes with diameters less than 200 Å (Figure 2b). The thickness could not be determined, but it is less than 30 Å. Comparison of Figure 2c with 2a, b, and d show that an increase in the ammonium concentration in the starting gel results in an increase in amorphous material. The particle size of the saponite flakes is not influenced by the ammonium concentration. The saponite synthesized at $H_2O/(Si + Al) = 25$ (280°C, HTSAP7a) consists of particles approximately 110 Å in thickness and 1100 Å in diameter, together with a few larger particles up to 6500 Å in diameter and 470 Å in thickness (Figure 2d).

The XRF results (Table 3) reveal a variation in bulk composition in the products due to the presence of amorphous material and corundum. Different concentrations of Mg, Al, and Si in the hydrothermal fluid are also reflected in the XRF bulk analyses. In all analyses, higher Al and lower Mg contents are observed in comparison with the theoretical composition (52.46 wt. % SiO_2, 15.72 wt. % Al_2O_3, 31.05 wt. % MgO, and 2.78 wt. % NH_4). An increase in the Si and Al content, together with a drop in the Mg content, is observed with decreasing temperature (Table 3). Based on the assumption that all magnesium is incorporated in the saponite, the XRF data reflect a relative increase in the amount of saponite in the products with increasing synthesis temperature (Figure 3).

ICP analyses of the hydrothermal fluid (Table 4) from runs up to 200°C are in agreement with the XRF

https://doi.org/10.1346/CCMN.1993.0410111 Published online by Cambridge University Press

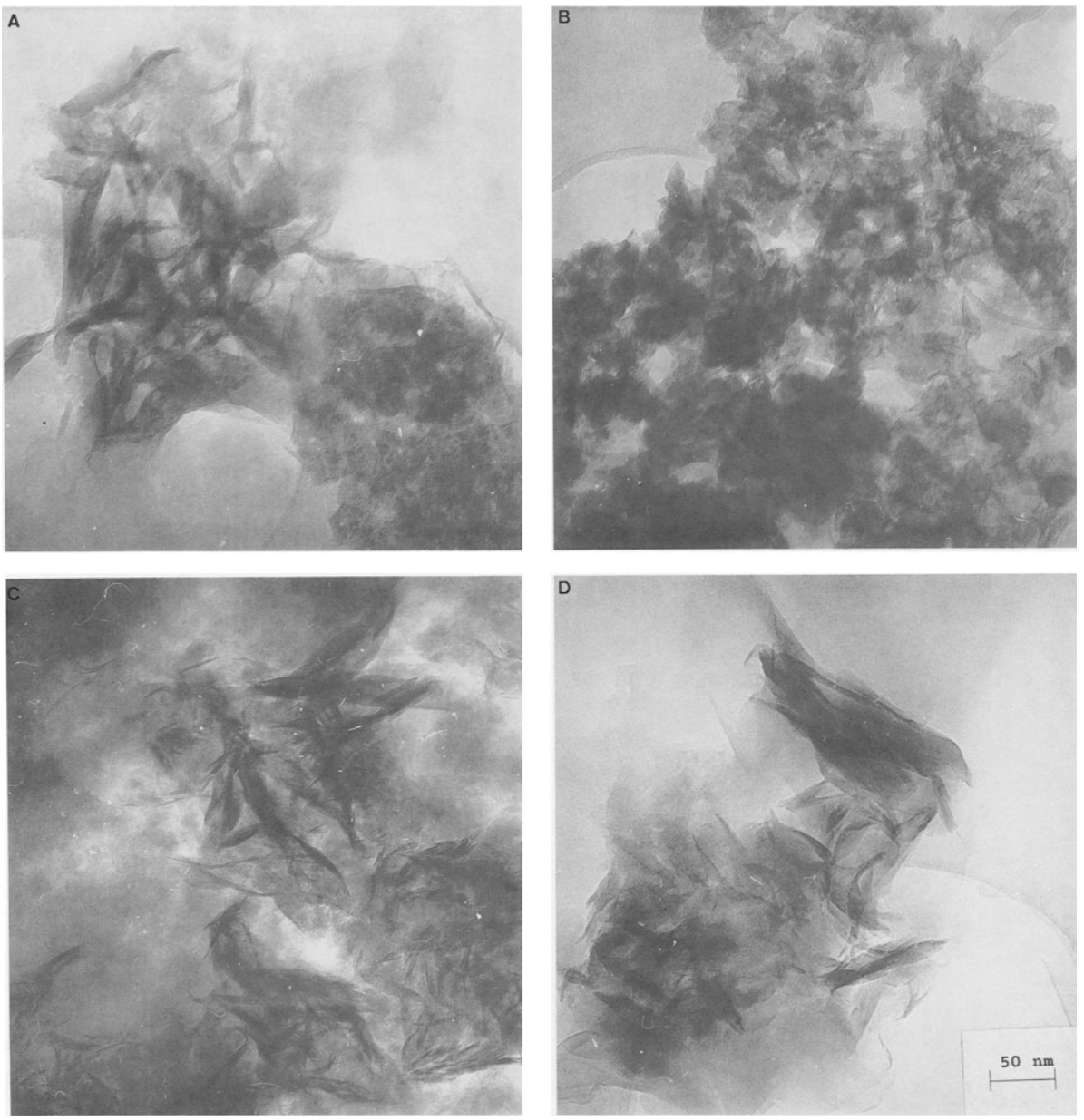

Figure 2. Transmission electron micrographs of saponites synthesized at: A) 280°C, $H_2O/(Si + Al) = 10$ and $NH_4/Al = 1.0$ (HTSAP2a); B) 125°C, $H_2O/(Si + Al) = 10$ and $NH_4/Al = 1.0$ (LTSAP2d); C) 280°C, $H_2O/(Si + Al) = 10$ and $NH_4/Al = 1.4$ (HTSAP4a); D) 280°C, $H_2O/(Si + Al) = 25$ and $NH_4/Al = 1.0$ (HTSAP7a).

analyses. The fluids contain higher Mg concentrations at lower synthesis temperatures.

Table 5 lists the infrared absorption maxima of the synthetic ammonium-saponite before and after calcination at 500°C, along with natural saponite (Krugersdorp Transvaal, van der Marel and Beutelspacher, 1976), and tobelite, an ammonium-mica (Voncken *et al.,* 1987). The observed absorption maxima of the synthetic saponite agree well with those of the natural saponite, although some Si-O vibrations are very weak or absent in the spectra of the synthetic saponite. The vibrations due to ammonium agree with the vibrations reported by Voncken *et al.* (1987) for ammonium-mica, although they are systematically shifted toward lower wave numbers.

TGA and DTA plots of HTSAP2a exhibit loss of water due to dehydration and dehydroxylation and loss of ammonia (Figure 4). During heating to 140°C, 6 wt. % of absorbed water is lost. The DTA curve shows an endothermic maximum at 100°C. In the range 140° to

https://doi.org/10.1346/CCMN.1993.0410111 Published online by Cambridge University Press

Table 3. X-ray fluorescence analyses of the run products bulk samples <64 μm (wt%). For comparison N analyses based on CEC determinations are given.

Sample	T (°C)	SiO_2	Al_2O_3	MgO	N	CEC run pr.	wt% sap.	CEC sap.
HTSAP2a	280	50.0	20.5	25.0	0.77	0.66	98	0.67
HTSAP2b	240	51.1	20.7	25.5	0.78	0.77	100	0.77
LTSAP2a	200	51.1	21.5	23.7	0.67	0.55	93	0.59
LTSAP2b	175	52.2	22.0	20.2	0.72	0.46	79	0.58
LTSAP2c	150	56.5	23.2	14.9	0.78	0.48	58	0.82
LTSAP2d	125	59.7	25.5	9.6	0.89	0.43	37	1.14
HTSAP7a	280	49.8	22.7	26.2	0.71	0.81	100	0.81
LTSAP7a	200	52.8	19.3	23.1	0.79	0.64	88	0.73
LTSAP7b	175	54.5	26.1	18.2	0.77	0.52	70	0.74
LTSAP7c	150	62.7	20.9	13.1	1.09	0.58	50	1.16
LTSAP7d	125	61.0	27.1	9.5	1.10	0.54	36	1.50
Theory[1]		52.5	15.7	31.1	2.16	2.16		

[1] Theoretical composition $(NH_4)_{0.6}Mg_3(Si_{3.4}Al_{0.6})O_{10}(OH)_2$.

525°C, an additional amount of 3 wt. % of chemically bound water is lost along with some ammonia. The gradual loss between 525°C and 750°C is interpreted as an overlap of ammonia loss and dehydration with dehydroxylation (Kloprogge *et al.*, 1990b). Between 750°C and 860°C, the dehydroxylation reaches its maximum weight loss of 2.8 wt. %. In the DTA plot, the dehydroxylation is represented by an endothermic peak with its maximum coming at 845°C, just before the exothermic peak, due to the breakdown of saponite at 875°C. No further weight loss is observed during breakdown.

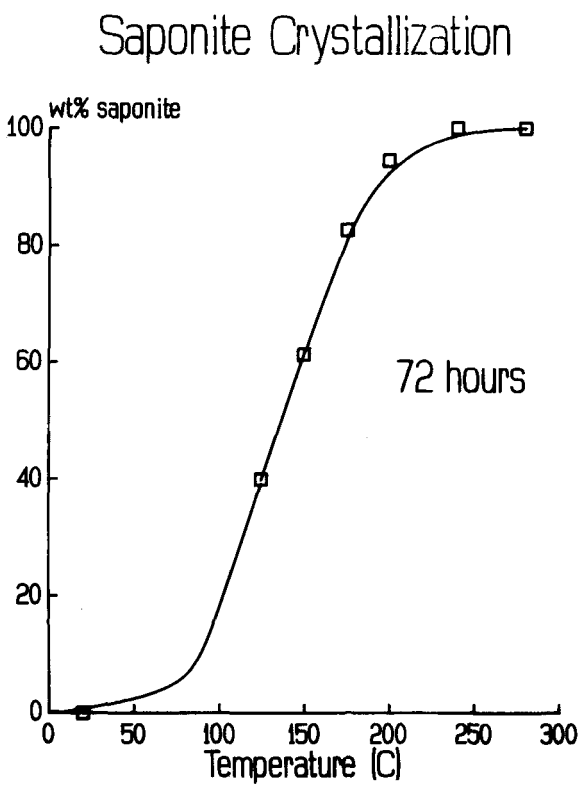

Figure 3. Weight percentage of saponite in the run product as a function of the synthesis temperature.

DISCUSSION

Saponite crystallinity

The synthesis of NH_4^+-saponite was successful in all experiments. The degree of crystallinity increased with increasing temperature as evidenced particularly by the increasing intensities of the (001) and (060) reflections in the diffractograms. Both TEM and sharpening of the XRD reflections, especially the (001) and (060), demonstrated an increasing crystallite size and a decreasing amount of amorphous material with higher synthesis temperatures. Higher ammonium concentrations in the starting gel influenced only the CEC of the product and the formation of amorphous material. Higher ammonium concentrations in the starting gel did not consistently affect the particle size, whereas an increase in the water content, as shown in Figures 2a and 2d, resulted in larger particles. It could be hypothesized that the higher ammonium concentration increases pH, increasing the solubility of silica from the gel, an effect that is even further increased during heating. This silica does not participate in the early stage of the crystallization of saponite. During crystallization, the pH drops and the silica is precipitated as amorphous material due to decreased solubility.

Table 4. Representative ICP analyses of the hydrothermal fluid.

Sample	T (°C)	Si ppm	Al ppm	Mg wt %
LTSAP6a	200	87	110	1.20
LTSAP6b	175	29	84	1.98
LTSAP6c	150	25	56	2.57
LTSAP6d	125	12	98	3.08

https://doi.org/10.1346/CCMN.1993.0410111 Published online by Cambridge University Press

Table 5. Infrared absorption maxima of ammonium-containing saponite HTSAP2a before and after calcination at 500°C, natural saponite, and synthetic tobelite.

HTSAP2a	HTSAP2a calcined 500°C	Saponite van der Marel and Beutelspacher (1976)	Tobelite Voncken *et al.* (1987)
3675	3675	3680 Si-O-H	
3625	3620	3625 (Mg)Al-O-H	3630 Al-O-H stretch
3440	3450	3420 H-O-H	
3260	3260		3300 NH_4 stretch
		3222 H-O-H	
3030			3070 NH_4 stretch
2840			2850 NH_4 stretch
1635	1635	1630 H-O-H	
1430			1430 NH_4 bending
1400			
		1103 Si-O	
		1058 Si-O/Si-O-Si	
1000	1000	1005 Si-O-Al	
835	840		
780	780	750 Si-O-Al	
740			
		693 Si-O-Al	
666	670	652 Si-O-Mg	
		610 Si-O	
528		528 Si-O-Al/Mg	
		480 Si-O	
		462 Si-O-Mg	
450	450	449 Si-O-Mg	425 Si-O

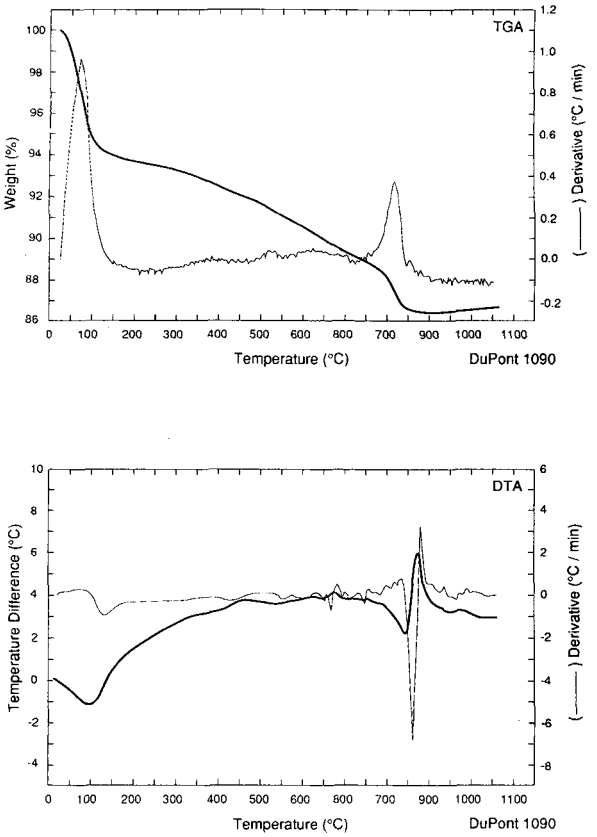

Figure 4. Thermogravimetric (upper) and differential thermal analyses of saponite (HTSAP2a).

The XRD spectra of the saponites synthesized by Iwasaki *et al.* (1989) indicate a very low crystallinity in comparison with our saponites due to their very short run times of 3 hr. Although Suquet *et al.* (1977) selected a run time of 15 days, a small, undetermined amount of amorphous material was still observed. As already stated by Koizumi and Roy (1959), it seems that, after a certain period, longer run times have no further effect either on the crystallite dimensions or on the saponite yield, indicating equilibrium. As we applied a run time of 3 days only, we cannot ascertain whether such a limiting time exists in our experiments.

The most crystalline material is obtained at 280°C, autogeneous water pressure (≈63 bar), and a H_2O/(Si + Al) ratio of 25. This temperature and the corresponding pressure agree well with those applied by Lipsicas *et al.* (1984) and Iwasaki *et al.* (1989). In contrast, Koizumi and Roy (1959) and Suquet *et al.* (1977) applied much higher pressures (1 kbar and 1.5 kbar, respectively).

Saponite chemistry

The theoretical structural formulae based on the starting mixture differ substantially from the observed chemical analyses and cation exchange capacities (Table 3). The chemical analyses indicate a considerably higher amount of aluminum. ^{27}Al MAS NMR data (Kloprogge, 1992; Kloprogge *et al.*, 1993b) show the presence of excess Al^{VI} within the interlayer or within octahedral sites of the saponite structure. The rather low CEC, based on exchangeable ammonium ions only, can be explained by the presence of Al^{3+} and/or Mg^{2+} as interlayer cations. Both possibilities are in agreement with the mass and charge balance. For example, ammonium-saponites with a theoretical structural formula of $(NH_4)_{0.27}Al_{0.11}(Mg)_3(Si_{3.4}Al_{0.6})O_{10}(OH)_2$ and $(NH_4)_{0.27}Mg_{0.165}(Mg_{2.835}Al_{0.11}vac_{0.055})(Si_{3.4}Al_{0.6})$-$O_{10}(OH)_2$ result in exactly the same mass and charge balance. ^{27}Al MAS-NMR did not provide conclusive evidence, because interlayer Al^{3+} exhibits a resonance at approximately the same frequency as the Al present in the octahedral layer (Kloprogge, 1992; Kloprogge *et al.*, 1993b). Saponites with Mg^{2+} within the interlayer sites have a basal spacing of 15.7 Å (Suquet *et al.*, 1977; Kloprogge, 1992; Kloprogge *et al.*, 1993a), which is larger than the observed basal spacing of approximately 12.3 Å. Therefore, the observed basal spacing and the doublet of the basal spacing after calcination, indicate that NH_4^+ and Al^{3+} ions reside on the exchange sites. The diffraction profile after calcination indicates the presence of H^+, Al^{3+}, and some remaining NH_4^+.

For the saponites produced at the higher synthesis temperatures (240°C and 280°C), the ammonium content of the products, based on the XRF data, are in

https://doi.org/10.1346/CCMN.1993.0410111 Published online by Cambridge University Press

reasonable agreement with the CEC values. At temperatures below 200°C, the CEC values are up to 50% lower than the XRF values (Table 3), indicating that ammonium resides within nonexchangeable sites, possibly of amorphous material, which is present in considerable amounts in the products of the runs performed at temperatures below 200°C.

Calculation of the magnesium distribution between the solid products after the NH_4Cl treatment and the coexisting hydrothermal fluid reveals that the amount of magnesium present in the hydrothermal fluid and in the solid state is equal to the total amount of magnesium in the gel. This is an additional indication that no Mg^{2+} was present as exchangeable cation. A too low amount of Mg should have been found in the analyses, as Mg is expected to be exchanged during the NH_4Cl treatment.

Crystallization model

^{27}Al MAS-NMR has shown that approximately 60% of the Al, which is initially octahedrally coordinated in aluminiumtriisopropylate, changes its coordination during gelation and is incorporated into the silica gel structure as tetrahedral Al (Kloprogge, 1992; Kloprogge *et al.,* 1993b). During synthesis, the pH decreases from approximately 10 to 4.5. In this pH and temperature range, the silica is only slightly soluble up to 1000 ppm. The Mg remains highly soluble within the entire pH range. Al, which is incorporated into the gel structure, is only slightly soluble; however, the Al not incorporated is highly soluble at high and low pH, though not in the neutral range. In agreement with the model for the crystallization of hectorite that Decarreau (1980) has proposed, it is suggested that crystallization of the saponite at temperatures above 150°C starts with the formation of tetrahedral layers with a certain amount of Al substitution, which is not fixed by the amount of tetrahedral Al in the gel. The initial ratio Si/Al of 5.67 and the Al^{IV}/Al^{VI} of 1.5 in the gel should result in a Si/Al^{IV} ratio of 9.44. However, values between 5 and 5.9 are observed in the products (Kloprogge, 1992; Kloprogge *et al.,* 1993b), indicating that Al^{VI} is dissolved from the gel and indicating the basic conditions of the hydrothermal fluid changes to Al^{IV}. At lower temperatures, the substitution is not only determined by the amount of tetrahedral Al in the gel and the hydrothermal solution but also by the amount of Al^{VI} captured in the amorphous phase. With higher synthesis temperatures, the rate of crystallization is higher. Syntheses at increasing temperatures and constant run times can be considered as equivalent to syntheses at increasing run times and constant temperatures. Assuming this equivalence, it is possible to propose a crystallization model based on the results of this study. The intensities of the (001) reflections increase, while the intensities of the other hk reflections remain nearly constant. Furthermore, the CEC of the saponite decreases with increasing synthesis temperature. These facts support the hypothesis that the crystallization initiates from separated sheets that later stack to form thicker saponite flakes. The sharpening of the XRD reflections, especially the (060), indicates that the lateral growth continues during stacking. During crystallization, pH decreases due to the formation of acetic acid. The remaining Mg together with a small amount of Al forms octahedral brucite (and gibbsite) layers upon the available tetrahedral layers. Both the XRF of the solid product and the ICP measurements of the hydrothermal fluid show that, during crystallization, an increasing amount of Mg is found in the product. Due to its small ionic radius combined with its high charge, the remaining Al is incorporated into the interlayer instead of NH_4. This model elucidates the lower $(Si/Al)^{IV}$ ratio observed with ^{29}Si MAS-NMR (Kloprogge, 1992; Kloprogge *et al.,* 1993b) as compared to the starting gel and the relatively high degree of Al substitution in the interlayer.

ACKNOWLEDGMENTS

The authors thank A. de Winter for his help and advice in the laboratory and T. Zalm for the TGA and DTA analyses. M. K. Titulaer is thanked for critically reviewing this manuscript.

REFERENCES

Decarreau, A. (1980) Cristallogène expérimentale des smectites magnésiennes: Hectorite, stevensite: *Bull. Mineral.* **103,** 579–590.

Decarreau, A. (1985) Partitioning of divalent transition elements between octahedral sheets of trioctahedral smectites and water: *Geochim. Cosmochim. Acta* **49,** 1537–1544.

Hamilton, D. L. and Henderson, C. M. B. (1968) The preparation of silicate compositions by a gelling method: *Mineral. Mag.* **36,** 832–838.

Hickson, D. A. (1974) Layered clay minerals, catalysts, and processes for using: *U.S. Patent* **3,844,979,** Oct. 29, 1974, 7 pp.

Hickson, D. A. (1975a) Layered clay minerals, catalysts, and processes for using: *U.S. Patent* **3,887,454,** June 3, 1975, 9 pp.

Hickson, D. A. (1975b) Layered clay minerals, catalysts, and processes for using: *U.S. Patent* **3,892,655,** July 1, 1975, 7 pp.

Iiyama, J. T. and Roy, R. (1963) Controlled synthesis of heteropolytypic (mixed layer) clay minerals: *Clays & Clay Minerals* **10,** 4–22.

Iwasaki, T., Onodera, Y., and Torii, K. (1989) Rheological properties of organophyllic synthetic hectorites and saponites: *Clays & Clay Minerals* **37,** 248–257.

Kloprogge, J. T. (1992) Pillared clays: preparation and characterization of clay minerals and aluminum-based pillaring agents: Ph.D. thesis, University of Utrecht, The Netherlands, *Geologica Ultraiectina* **91,** pp #s.

Kloprogge, J. T., van der Eerden, A. M. J., Jansen, J. B. H., and Geus, J. W. (1990a) Hydrothermal synthesis of Na-beidellite: *Geologie en Mijnbouw,* **69,** 351–357.

Kloprogge, J. T., Jansen, J. B. H., and Geus, J. W. (1990b) Characterization of synthetic Na-beidellite: *Clays & Clay Minerals* **38,** 409–414.

Kloprogge, J. T., Breukelaar, J., Geus, J. W., and Jansen, J.

B. H. (1993a) Properties of synthetic saponites in relation to different interlayer cations: Na^+, K^+, Rb^+, Ca^{2+}, Ba^{2+}, Ce^{4+}: *Clays & Clay Minerals,* in press.

Kloprogge, J. T., Breukelaar, J., Wilson, A. E., Geus, J. W., and Jansen, J. B. H. (1993b) Solid-state nuclear magnetic resonance spectroscopy on synthetic saponites: aluminum on the interlayer site: *Clays & Clay Minerals,* in press.

Koizumi, M. and Roy, R. (1959) Synthetic montmorillonoids with variable exchange capacity: *Amer. Mineral.* **44,** 788–805.

Lipsicas, M., Raythatha, R. H., Pinnavaia, T. J., Johnson, I. D., Giese Jr., R. F., Costanzo, P. M., and Roberts, J.-L. (1984) Silicon and aluminium site distributions in 2:1 layered silicate clays: *Nature* **309,** 604–607.

Plee, D., Gatineau, L., and Fripiat, J. J. (1987) Pillaring processes of smectites with and without tetrahedral substitution: *Clays & Clay Minerals* **35,** 81–88.

Schutz, A., Stone, W. E. E., Poncelet, G., and Fripiat, J. J. (1987) Preparation and characterization of bidimensional zeolitic structures obtained from synthetic beidellite and hydroxy-aluminum solutions: *Clays & Clay Minerals* **35,** 251–261.

Shabtai, J., Rosell, M., and Tokarz, M. (1984) Cross-linked smectites. III. Synthesis and properties of hydroxy-aluminum hectorites and fluorhectorites: *Clays & Clay Minerals* **32,** 99–107.

Sterte, J. and Shabtai, J. (1987) Cross-linked smectites. V. Synthesis and properties of hydroxy-silicoaluminum montmorillonites and fluorhectorites: *Clays & Clay Minerals* **35,** 429–439.

Suquet, H., Iiyama, J. T., Kodama, H., and Pezerat, H. (1977) Synthesis and swelling properties of saponites with increasing layer charge: *Clays & Clay Minerals* **25,** 231–242.

Suquet H., de la Calle, and Pezerat, H. (1975) Swelling and structural organization of saponite: *Clays & Clay Minerals* **23,** 1–9.

Torii, K. and Iwasaki, T. (1987) Synthesis of hectorite: *Clay Science* **7,** 1–16.

Van der Marel, H. W. and Beutelspacher, H. (1976) *Atlas of Infrared Spectroscopy of Clay Minerals and their Admixtures:* Elsevier, Amsterdam.

Voncken, J. H. L., Wevers, J. M. A. R., van der Eerden, A. M. J., Bos, A., and Jansen, J. B. H. (1987) Hydrothermal synthesis of tobelite, $NH_4Al_2Si_3O_{10}(OH)_2$, from various starting materials and implications for its occurrence in nature: *Geologie en Mijnbouw* **66,** 259–269.

Woessner, D. E. (1989) Characterization of clay minerals by ^{27}Al nuclear magnetic resonance spectroscopy: *Amer. Mineral.* **74,** 203–215.

(Received 23 September 1992; accepted 12 January 1993; Ms. 2275)